Exact solution of reflection coefficient in reservoirs with tilted fractures

Huaizhen Chen, Kristopher Innanen

ABSTRACT

We first present detailed expressions of polarization vectors of P- and SV-waves for a transversely isotropic medium with a tilted symmetry axis (TTI) as a function of stiffness parameters of a transversely isotropic medium with a vertical symmetry axis (VTI), and then we propose the equation to calculate the exact solution of PP-wave reflection coefficient in TTI media. In order to relate the stiffness matrix of TTI media to fracture properties (e.g. fracture density and fillings moduli), we use the stiffness matrix of HTI media given by the linear slip theory to obtain the stiffness matrix of VTI media using the Bond rotation, which provides us to calculate stiffness parameters for TTI media given different fracture properties and tilted angles. We also study how to compute the transmission angle in TTI media using the extended Snell′s law. We finally model PP-wave reflection coefficient variations with the incidence angle and the azimuthal angle given different values of fracture density and tilted angle. We conclude that in the case of TI media with a high tilted angle, the tilted angle mainly affects the value of the reflection coefficient, while the fracture density affects the variation of reflection coefficient with the azimuthal angle.

INTRODUCTION

Seismic wave propagation in most subsurface layers exhibits phenomenon of anisotropy, and transverse isotropy (TI) is a common anisotropic model used for characterization of seismic wave propagation (Alkhalifah and Larner, 1994; Alkhalifah, 1995; Grechka et al., 2001; Bakulin et al., 2010; Wang and Tsvankin, 2013). A rock with a set of parallel vertical fractures is equivalent to a horizontal transversely isotropic (HTI) medium (Schoenberg and Douma, 1988; Schoenberg and Sayers, 1995; Bakulin et al., 2000; Chen et al., 2014, 2017), and a finely layered shale rock with a vertical or sub-vertical symmetry axis is considered to be a vertical transversely isotropic (VTI) medium (Thomsen, 1986; Carcione, 1992; Berryman et al., 1999; Carcione, 2000; Stovas et al., 2006). The TI medium with a tilted symmetry axis (TTI media) is considered to include two cases: the finely layered shale with a tilted angle, and a vertically fractured rock with a tilted symmetry axis (Behera and Tsvankin, 2009; Fletcher et al., 2009; Nadri et al., 2012; Stovas and Alkhalifah, 2013; Wang and Tsvankin, 2013; Wang and Peng, 2015; Shragge, 2016). In the present study, we focus on the TTI media formed by rotating the vertically fractured rock.

The Zoeppritz equation is proposed to describe how seismic wave energy partitions at an interface, which is well used to measure exact reflection and transmission coefficients of seismic wave (Shuey, 1985; Sheriff and Geldart, 1995; Aki and Richards, 2002; Avseth et al., 2010). The Zoeppritz equation has been extended to weakly anisotropic media to compute exact solutions of seismic wave transmission and reflection coefficients (Schoenberg and Protázio, 1992; Rüger, 1996; Pšenčík and Vavryčuk, 1998). The quantities required to compute for the calculation of exact solutions of reflection coefficients in weakly anisotropic media involve polarization vectors and azimuthal angles (Thomsen,

1988; Tsvankin, 1997; Pšenčík and Gajewski, 1998), which are related to stiffness parameters. Hudson (1980) presented a penny-shaped crack model to study how cracks affect the elastic matrix of anisotropic rocks. For rocks containing a set of vertical and rotationally invariant fractures, the linear slip theory Schoenberg and Douma (1988); Schoenberg and Sayers (1995) is used to express the influence of fractures on the total property of fractured rocks as a function of the normal and tangential fracture weaknesses. Combining the penny-shaped crack model and the linear slip theory, Bakulin et al. (2000) related the fracture weaknesses to fracture properties (e.g. fracture density and aspect ratio).

In this study, using the stiffness matrix of HTI media (Schoenberg and Sayers, 1995; Bakulin et al., 2000; Gurevich, 2003), we first write the stiffness matrix of VTI media in terms of the normal and tangential fracture weaknesses using the Bond transformation Auld (1990) and assuming the tilted angle to be $\pi/2$, and then we obtain the explicit expressions of stiffness parameters of TTI media as a function of fracture weaknesses. After calculating polarization vectors and azimuthal angles of P- and SV-waves for TTI media, we compute the exact solution of PP-wave reflection coefficient using the extended Zoeppritz equation. We finally analyze how PP-wave exact reflection coefficient varies with the incidence angle and the azimuthal angle given different values of fracture density and tilted angle.

THEORY AND METHOD

Polarization and azimuthal angles of P- and SV-wave in an anisotropic medium

In the case of a TI medium with a tilted angle (TTI), a harmonic plan wave incident from the half-space may generate three reflected and three transmitted waves (Pšenčík and Vavryčuk, 1998), as shown in Figure 1. In the present study, we focus on P- and SV-wave reflection and transmission in the TTI medium.

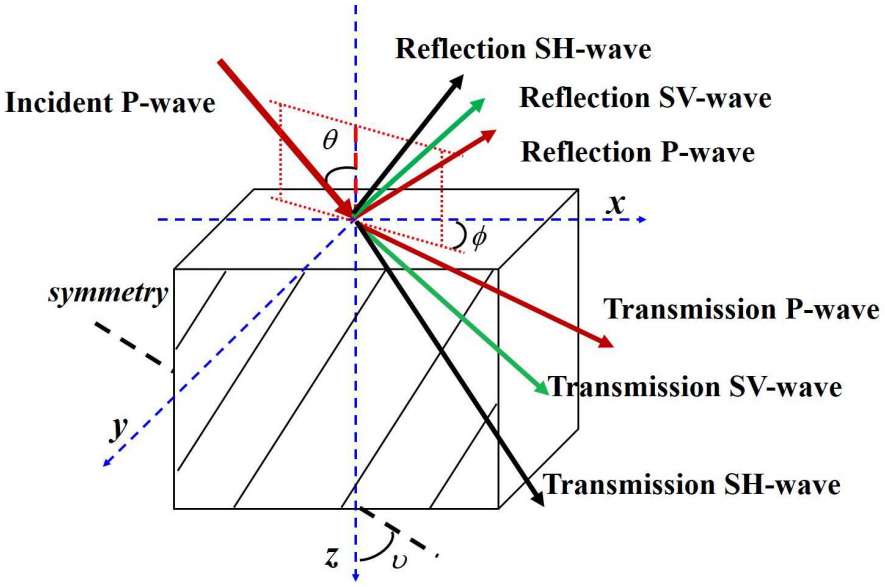

FIG. 1. Incident P-wave generating three reflection waves and three transmission waves in a TTI medium. The quantities θ, ϕ, and υ denote the P-wave incidence angle, the azimuthal angle, and the tilted angle.

Polarization vectors of P-and SV-waves are given by

$$\begin{aligned} \mathrm{P_P} &= \left[\sin\alpha_{\mathrm{P}}\cos\beta_{\mathrm{P}}, \sin\alpha_{\mathrm{P}}\sin\beta_{\mathrm{P}}, \cos\alpha_{\mathrm{P}}\right], \\ \mathrm{P_{SV}} &= \left[\sin\alpha_{\mathrm{SV}}\cos\beta_{\mathrm{SV}}, \sin\alpha_{\mathrm{SV}}\sin\beta_{\mathrm{SV}}, -\sin\alpha_{\mathrm{SV}}\right], \end{aligned} \tag{1}$$

where α and β are the polarization and azimuthal angles of the wave, respectively.

For the P-wave, α_{P} and β_{P} are expressed as

$$\begin{aligned} \alpha_{\mathrm{P}}&=\arccos\left[\frac{p_z^{\mathrm{P}}}{\sqrt{\left(p_x^{\mathrm{P}}\right)^2+\left(p_y^{\mathrm{P}}\right)^2+\left(p_z^{\mathrm{P}}\right)^2}}\right], \\ \beta_{\mathrm{P}}&=\arctan\left(\frac{p_y^{\mathrm{P}}}{p_x^{\mathrm{P}}}\right), \end{aligned} \tag{2}$$

where

$$\begin{aligned} p_x^{\mathrm{P}} =&\frac{1}{L_{\mathrm{P}}}\{2\left(C_{13}^{\mathrm{V}}+C_{44}^{\mathrm{V}}\right)GE\cos\upsilon \\ &+\left[\left(C_{11}^{\mathrm{V}}-C_{44}^{\mathrm{V}}\right)\left(E^2+F^2\right)-\left(C_{33}^{\mathrm{V}}-C_{44}^{\mathrm{V}}\right)G^2-\sqrt{D}\right]\sin\upsilon\}, \end{aligned}$$

$$p_y^{\mathrm{P}} =\frac{1}{L_{\mathrm{P}}}\left\{2\left(C_{13}^{\mathrm{V}}+C_{44}^{\mathrm{V}}\right)GF\right\},$$

$$\begin{aligned} p_z^{\mathrm{P}} =&\frac{1}{L_{\mathrm{P}}}\{2\left(C_{13}^{\mathrm{V}}+C_{44}^{\mathrm{V}}\right)GE\sin\upsilon \\ &-\left[\left(C_{11}^{\mathrm{V}}-C_{44}^{\mathrm{V}}\right)\left(E^2+F^2\right)-\left(C_{33}^{\mathrm{V}}-C_{44}^{\mathrm{V}}\right)G^2-\sqrt{D}\right]\sin\upsilon\}, \end{aligned}$$

$$\begin{aligned} L_{\mathrm{P}} =&\{4\left(C_{13}^{\mathrm{V}}+C_{44}^{\mathrm{V}}\right)^2G^2\left(E^2+F^2\right) \\ &+\left[\left(C_{11}^{\mathrm{V}}-C_{44}^{\mathrm{V}}\right)\left(E^2+F^2\right)-\left(C_{33}^{\mathrm{V}}-C_{44}^{\mathrm{V}}\right)G^2-\sqrt{D}\right]^2\}^{1/2}, \end{aligned}$$

$$D =\left[\left(C_{11}^{\mathrm{V}}-C_{44}^{\mathrm{V}}\right)\left(E^2+F^2\right)-\left(C_{33}^{\mathrm{V}}-C_{44}^{\mathrm{V}}\right)G^2\right]^2+4\left(C_{13}^{\mathrm{V}}+C_{44}^{\mathrm{V}}\right)\left(E^2+F^2\right)^2G^2,$$

$$E =\sin\theta\cos\upsilon\cos\phi+\cos\theta\sin\upsilon,$$

$$F =\sin\theta\sin\phi,$$

$$G = -\sin\theta\sin\upsilon\cos\phi + \cos\theta\cos\upsilon, \tag{3}$$

and where C_{11}^{V}, C_{13}^{V}, C_{33}^{V} and C_{44}^{V} are stiffness parameters of the TI medium with a vertical symmetry axis (VTI), which means that a TTI medium can be described by rotating a VTI medium.

For the SV-wave, α_{SV} and β_{SV} are given by

$$\begin{aligned}
\alpha_{\mathrm{SV}}&=\arccos\left[\frac{p_z^{\mathrm{SV}}}{\sqrt{\left(p_x^{\mathrm{SV}}\right)^2+\left(p_y^{\mathrm{SV}}\right)^2+\left(p_z^{\mathrm{SV}}\right)^2}}\right],\\
\beta_{\mathrm{SV}}&=\arctan\left(\frac{p_y^{\mathrm{SV}}}{p_x^{\mathrm{SV}}}\right),
\end{aligned} \tag{4}$$

where

$$\begin{aligned}
p_x^{\mathrm{SV}} = \frac{1}{L_{\mathrm{SV}}}\{&2\left(C_{13}^{\mathrm{V}}+C_{44}^{\mathrm{V}}\right)GE\cos\upsilon\\
&+\left[\left(C_{11}^{\mathrm{V}}-C_{44}^{\mathrm{V}}\right)\left(E^2+F^2\right)-\left(C_{33}^{\mathrm{V}}-C_{44}^{\mathrm{V}}\right)G^2+\sqrt{D}\right]\sin\upsilon\},
\end{aligned}$$

$$p_y^{\mathrm{SV}} = \frac{1}{L_{\mathrm{SV}}}\left\{2\left(C_{13}^{\mathrm{V}}+C_{44}^{\mathrm{V}}\right)GF\right\},$$

$$\begin{aligned}
p_z^{\mathrm{SV}} = \frac{1}{L_{\mathrm{SV}}}\{&2\left(C_{13}^{\mathrm{V}}+C_{44}^{\mathrm{V}}\right)GE\sin\upsilon\\
&-\left[\left(C_{11}^{\mathrm{V}}-C_{44}^{\mathrm{V}}\right)\left(E^2+F^2\right)-\left(C_{33}^{\mathrm{V}}-C_{44}^{\mathrm{V}}\right)G^2+\sqrt{D}\right]\sin\upsilon\},
\end{aligned}$$

$$\begin{aligned}
L_{\mathrm{SV}} = \{&4\left(C_{13}^{\mathrm{V}}+C_{44}^{\mathrm{V}}\right)^2G^2\left(E^2+F^2\right)\\
&+\left[\left(C_{11}^{\mathrm{V}}-C_{44}^{\mathrm{V}}\right)\left(E^2+F^2\right)-\left(C_{33}^{\mathrm{V}}-C_{44}^{\mathrm{V}}\right)G^2+\sqrt{D}\right]^2\}^{1/2}.
\end{aligned} \tag{5}$$

Exact solution of reflection coefficient in anisotropic media

Extend Zoeppritz equation can be used to obtain exact solution of the reflection coefficient in anisotropic media (Schoenberg and Protázio, 1992; Pšenčík and Vavryčuk, 1998). For the TTI media, the extended Zoeppritz equation is given by

$$\begin{bmatrix} X_{11} & X_{12} & X_{13} & X_{14}\\ X_{21} & X_{22} & X_{23} & X_{24}\\ X_{31} & X_{32} & X_{33} & X_{34}\\ X_{41} & X_{42} & X_{43} & X_{44}\end{bmatrix}\begin{bmatrix} R_{\mathrm{PP}}\\ R_{\mathrm{PSV}}\\ T_{\mathrm{PP}}\\ T_{\mathrm{PSV}}\end{bmatrix} = \begin{bmatrix} Y_1\\ Y_2\\ Y_3\\ Y_4\end{bmatrix}, \tag{6}$$

where $R_{\rm PP}$ and $R_{\rm PSV}$ are PP-and PSV-wave reflection coefficients, $T_{\rm PP}$ and $T_{\rm PSV}$ are PP-and PSV-wave transmission coefficients, and where

$$X_{11} = \sin\alpha_P^{\rm U}\cos\beta_P^{\rm U}, X_{12} = \cos\alpha_{SV}^{U}\cos\beta_{SV}^{U}, X_{13} = -\sin\alpha_{\rm P}^{L}\cos\beta_{\rm P}^{L}, X_{14} = -\cos\alpha_{\rm SV}^{L}\cos\beta_{\rm SV}^{L},$$

$$X_{21} = \cos\alpha_{\rm P}^{\rm U}, X_{22} = -\sin\alpha_{\rm SV}^{\rm U}, X_{23} = \cos\alpha_{\rm P}^{\rm L}, X_{24} = -\sin\alpha_{\rm SV}^{\rm L},$$

$$X_{31} = -\frac{1}{V_{\rm P}^{\rm U}}[C_{13}^{\rm U}\sin\alpha_{\rm P}^{\rm U}\cos\beta_{\rm P}^{\rm U}\sin\theta_{\rm P}^{\rm U}\cos\phi + C_{23}^{\rm U}\sin\alpha_{\rm P}^{\rm U}\cos\beta_{\rm P}^{\rm U}\sin\theta_{\rm P}^{\rm U}\sin\phi + C_{33}^{\rm U}\sin\alpha_{\rm P}^{\rm U}\cos\theta_{\rm P}^{\rm U} - C_{35}^{\rm U}\left(\sin\alpha_{\rm P}^{\rm U}\cos\beta_{\rm P}^{\rm U}\cos\theta_{\rm P}^{\rm U} + \cos\alpha_{\rm P}^{\rm U}\sin\theta_{\rm P}^{\rm U}\cos\phi\right)],$$

$$X_{32} = -\frac{1}{V_{\rm SV}^{\rm U}}[C_{13}^{\rm U}\cos\alpha_{\rm SV}^{\rm U}\cos\beta_{\rm SV}^{\rm U}\sin\theta_{\rm SV}^{\rm U}\cos\phi + C_{23}^{\rm U}\cos\alpha_{\rm SV}^{\rm U}\sin\beta_{\rm SV}^{\rm U}\sin\theta_{\rm SV}^{\rm U}\sin\phi - C_{33}^{\rm U}\sin\alpha_{\rm SV}^{\rm U}\cos\theta_{\rm SV}^{\rm U}+C_{35}^{\rm U}\left(-\cos\alpha_{\rm SV}^{\rm U}\cos\beta_{\rm SV}^{\rm U}\cos\theta_{\rm SV}^{\rm U} + \sin\alpha_{\rm SV}^{\rm U}\sin\theta_{\rm SV}^{\rm U}\cos\phi\right)],$$

$$X_{33} = \frac{1}{V_{\rm P}^{\rm L}}[C_{13}^{\rm L}\sin\alpha_{\rm P}^{\rm L}\cos\beta_{\rm P}^{\rm L}\sin\theta_{\rm P}^{\rm L}\cos\phi + C_{23}^{\rm L}\sin\alpha_{\rm P}^{\rm L}\sin\beta_{\rm P}^{\rm L}\sin\theta_{\rm P}^{\rm L}\sin\phi + C_{33}^{\rm L}\cos\alpha_{\rm P}^{\rm L}\cos\theta_{\rm P}^{\rm L} + C_{35}^{\rm L}\left(\sin\alpha_{\rm P}^{\rm L}\cos\beta_{\rm P}^{\rm L}\cos\theta_{\rm P}^{\rm L} + \cos\alpha_{\rm P}^{\rm L}\sin\theta_{\rm P}^{\rm L}\cos\phi\right)],$$

$$X_{34} = \frac{1}{V_{\rm SV}^{\rm L}}[C_{13}^{\rm L}\cos\alpha_{\rm SV}^{\rm L}\cos\beta_{\rm SV}^{\rm L}\sin\theta_{\rm SV}^{\rm L}\cos\phi + C_{23}^{\rm L}\cos\alpha_{\rm SV}^{\rm L}\sin\beta_{\rm SV}^{\rm L}\sin\theta_{\rm SV}^{\rm L}\sin\phi - C_{33}^{\rm L}\sin\alpha_{\rm SV}^{\rm L}\cos\theta_{\rm SV}^{\rm L}+C_{35}^{\rm L}\left(\cos\alpha_{\rm SV}^{\rm L}\cos\beta_{\rm SV}^{\rm L}\cos\theta_{\rm SV}^{\rm L} - \sin\alpha_{\rm SV}^{\rm L}\sin\theta_{\rm SV}^{\rm L}\cos\phi\right)],$$

$$X_{41} = -\frac{1}{V_{\rm P}^{\rm U}}[C_{15}^{\rm U}\sin\alpha_{\rm P}^{\rm U}\cos\beta_{\rm P}^{\rm U}\sin\theta_{\rm P}^{\rm U}\cos\phi + C_{25}^{\rm U}\sin\alpha_{\rm P}^{\rm U}\sin\beta_{\rm P}^{\rm U}\sin\theta_{\rm P}^{\rm U}\sin\phi + C_{35}^{\rm U}\cos\alpha_{\rm P}^{\rm U}\cos\theta_{\rm P}^{\rm U} - C_{55}^{\rm U}(\sin\alpha_{\rm P}^{\rm U}\cos\beta_{\rm P}^{\rm U}\cos\theta_{\rm P}^{\rm U} + \cos\alpha_{\rm P}^{\rm U}\sin\theta_{\rm P}^{\rm U}\cos\phi)],$$

$$X_{42} = -\frac{1}{V_{\rm SV}^{\rm U}}[C_{15}^{\rm U}\cos\alpha_{\rm SV}^{\rm U}\cos\beta_{\rm SV}^{\rm U}\sin\theta_{\rm SV}^{\rm U}\cos\phi + C_{25}^{\rm U}\cos\alpha_{\rm SV}^{\rm U}\sin\beta_{\rm SV}^{\rm U}\sin\theta_{\rm SV}^{\rm U}\sin\phi - C_{35}^{\rm U}\sin\alpha_{\rm SV}^{\rm U}\cos\theta_{\rm SV}^{\rm U} + C_{55}^{\rm U}(-\cos\alpha_{\rm SV}^{\rm U}\cos\beta_{\rm SV}^{\rm U}\cos\theta_{\rm SV}^{\rm U} + \sin\alpha_{\rm SV}^{\rm U}\sin\theta_{\rm SV}^{\rm U}\cos\phi)],$$

$$X_{43} = \frac{1}{V_{\rm P}^{\rm L}}[C_{15}^{\rm L}\sin\alpha_{\rm P}^{\rm L}\cos\beta_{\rm P}^{\rm L}\sin\theta_{\rm P}^{\rm L}\cos\phi + C_{25}^{\rm L}\sin\alpha_{\rm P}^{\rm L}\sin\beta_{\rm P}^{\rm L}\sin\theta_{\rm P}^{\rm L}\sin\phi + C_{35}^{\rm L}\cos\alpha_{\rm P}^{\rm L}\cos\theta_{\rm P}^{\rm L} + C_{55}^{\rm L}(\sin\alpha_{\rm P}^{\rm L}\cos\beta_{\rm P}^{\rm L}\cos\theta_{\rm P}^{\rm L} + \cos\alpha_{\rm P}^{\rm L}\sin\theta_{\rm P}^{\rm L}\cos\phi)],$$

$$X_{44} = \frac{1}{V_{\rm SV}^{\rm L}}[C_{15}^{\rm L}\cos\alpha_{\rm SV}^{\rm L}\cos\beta_{\rm SV}^{\rm L}\sin\theta_{\rm SV}^{\rm L}\cos\phi + C_{25}^{\rm L}\cos\alpha_{\rm SV}^{\rm L}\sin\beta_{\rm SV}^{\rm L}\sin\theta_{\rm SV}^{\rm L}\sin\phi - C_{35}^{\rm L}\sin\alpha_{\rm SV}^{\rm L}\cos\theta_{\rm SV}^{\rm L} + C_{55}^{\rm L}(\cos\alpha_{\rm SV}^{\rm L}\cos\beta_{\rm SV}^{\rm L}\cos\theta_{\rm SV}^{\rm L} - \sin\alpha_{\rm SV}^{\rm L}\sin\theta_{\rm SV}^{\rm L}\cos\phi)],$$

$$Y_1 = -\sin\alpha_{i\mathrm{P}}^{\mathrm{U}}\cos\beta_{i\mathrm{P}}^{\mathrm{U}},$$

$$Y_2 = \cos\alpha_{i\mathrm{P}}^{\mathrm{U}},$$

$$\begin{aligned} Y_3 = \frac{1}{V_{i\mathrm{P}}^{\mathrm{U}}}[&C_{13}^{\mathrm{U}}\sin\alpha_{i\mathrm{P}}^{\mathrm{U}}\cos\beta_{i\mathrm{P}}^{\mathrm{U}}\sin\theta_{i\mathrm{P}}^{\mathrm{U}}\cos\phi + C_{23}^{\mathrm{U}}\sin\alpha_{i\mathrm{P}}^{\mathrm{U}}\sin\beta_{i\mathrm{P}}^{\mathrm{U}}\sin\theta_{i\mathrm{P}}^{\mathrm{U}}\sin\phi \\ &+ C_{33}^{\mathrm{U}}\cos\alpha_{i\mathrm{P}}^{\mathrm{U}}\cos\theta_{i\mathrm{P}}^{\mathrm{U}} + C_{35}^{\mathrm{U}}\left(\sin\alpha_{i\mathrm{P}}^{\mathrm{U}}\cos\beta_{i\mathrm{P}}^{\mathrm{U}}\cos\theta_{i\mathrm{P}}^{\mathrm{U}} + \cos\alpha_{i\mathrm{P}}^{\mathrm{U}}\sin\theta_{i\mathrm{P}}^{\mathrm{U}}\cos\phi\right)], \end{aligned}$$

$$\begin{aligned} Y_4 = \frac{1}{V_{i\mathrm{P}}^{\mathrm{U}}}[&C_{15}^{\mathrm{U}}\sin\alpha_{i\mathrm{P}}^{\mathrm{U}}\cos\beta_{i\mathrm{P}}^{\mathrm{U}}\sin\theta_{i\mathrm{P}}^{\mathrm{U}}\cos\phi + C_{25}^{\mathrm{U}}\sin\alpha_{i\mathrm{P}}^{\mathrm{U}}\sin\beta_{i\mathrm{P}}^{\mathrm{U}}\sin\theta_{i\mathrm{P}}^{\mathrm{U}}\sin\phi \\ &+ C_{35}^{\mathrm{U}}\cos\alpha_{i\mathrm{P}}^{\mathrm{U}}\cos\theta_{i\mathrm{P}}^{\mathrm{U}} + C_{55}^{\mathrm{U}}(\sin\alpha_{i\mathrm{P}}^{\mathrm{U}}\cos\beta_{i\mathrm{P}}^{\mathrm{U}}\cos\theta_{i\mathrm{P}}^{\mathrm{U}} + \cos\alpha_{i\mathrm{P}}^{\mathrm{U}}\sin\theta_{i\mathrm{P}}^{\mathrm{U}}\cos\phi)], \end{aligned} \tag{7}$$

where V_{P} and V_{SV} are P-and SV-wave velocities, iP represents the incidence P-wave, C_{13}, C_{15}, C_{23}, C_{25}, C_{33}, C_{35} and C_{55} are stiffness parameters of TTI media, and the superscripts U and cL denote the upper and lower TTI layers.

We write equation 6 succinctly as

$$\mathbf{XR} = \mathbf{Y}, \tag{8}$$

where $\mathbf{X}$ represents the displacement-stress matrix for the reflected and transmitted waves, $\mathbf{R}$ is the reflection and transmission coefficients vector, and $\mathbf{Y}$ is the displacement-stress vector of the incident P-wave, respectively. Hence, the reflection and transmission coefficient vector is calculated by

$$\mathbf{R} = (\mathbf{X})^{-1}\,\mathbf{Y}. \tag{9}$$

Relationships between stiffness matrices of anisotropic media

The stiffness matrix of the TTI medium is obtained using the VTI medium stiffness matrix and the Bond transformation (Auld, 1990)

$$\begin{aligned} \mathbf{C}_{\mathrm{TTI}} &= \begin{bmatrix} C_{11} & C_{12} & C_{13} & C_{14} & C_{15} & C_{16} \\ C_{21} & C_{22} & C_{23} & C_{24} & C_{25} & C_{26} \\ C_{31} & C_{32} & C_{33} & C_{34} & C_{35} & C_{36} \\ C_{41} & C_{42} & C_{43} & C_{44} & C_{45} & C_{46} \\ C_{51} & C_{52} & C_{53} & C_{54} & C_{55} & C_{56} \\ C_{61} & C_{62} & C_{63} & C_{64} & C_{65} & C_{66} \end{bmatrix} = \mathbf{M}_{\upsilon}\mathbf{C}_{\mathrm{VTI}}\mathbf{M}_{\upsilon}^{T} \\ &= \mathbf{M}_{\upsilon} \begin{bmatrix} C_{11}^{\mathrm{V}} & C_{12}^{\mathrm{V}} & C_{13}^{\mathrm{V}} & C_{14}^{\mathrm{V}} & C_{15}^{\mathrm{V}} & C_{16}^{\mathrm{V}} \\ C_{21}^{\mathrm{V}} & C_{22}^{\mathrm{V}} & C_{23}^{\mathrm{V}} & C_{24}^{\mathrm{V}} & C_{25}^{\mathrm{V}} & C_{26}^{\mathrm{V}} \\ C_{31}^{\mathrm{V}} & C_{32}^{\mathrm{V}} & C_{33}^{\mathrm{V}} & C_{34}^{\mathrm{V}} & C_{35}^{\mathrm{V}} & C_{36}^{\mathrm{V}} \\ C_{41}^{\mathrm{V}} & C_{42}^{\mathrm{V}} & C_{43}^{\mathrm{V}} & C_{44}^{\mathrm{V}} & C_{45}^{\mathrm{V}} & C_{46}^{\mathrm{V}} \\ C_{51}^{\mathrm{V}} & C_{52}^{\mathrm{V}} & C_{53}^{\mathrm{V}} & C_{54}^{\mathrm{V}} & C_{55}^{\mathrm{V}} & C_{56}^{\mathrm{V}} \\ C_{61}^{\mathrm{V}} & C_{62}^{\mathrm{V}} & C_{63}^{\mathrm{V}} & C_{64}^{\mathrm{V}} & C_{65}^{\mathrm{V}} & C_{66}^{\mathrm{V}} \end{bmatrix} \mathbf{M}_{\upsilon}^{T}, \end{aligned} \tag{10}$$

where

$$\mathbf{M}_{\upsilon} = \begin{bmatrix} \cos^2\upsilon & 0 & \sin^2\upsilon & 0 & -\sin 2\upsilon & 0 \\ 0 & 1 & 0 & 0 & 0 & 0 \\ \sin^2\upsilon & 0 & \cos^2\upsilon & 0 & \sin 2\upsilon & 0 \\ 0 & 0 & 0 & \cos\upsilon & 0 & \sin\upsilon \\ \frac{1}{2}\sin 2\upsilon & 0 & -\frac{1}{2}\sin 2\upsilon & 0 & \cos 2\upsilon & 0 \\ 0 & 0 & 0 & -\sin\upsilon & 0 & \cos\upsilon \end{bmatrix}, \tag{11}$$

and

$$\mathbf{M}_{\upsilon}^{T} = \begin{bmatrix} \cos^2\upsilon & 0 & \sin^2\upsilon & 0 & \frac{1}{2}\sin 2\upsilon & 0 \\ 0 & 1 & 0 & 0 & 0 & 0 \\ \sin^2\upsilon & 0 & \cos^2\upsilon & 0 & -\frac{1}{2}\sin 2\upsilon & 0 \\ 0 & 0 & 0 & \cos\upsilon & 0 & -\sin\upsilon \\ -\sin 2\upsilon & 0 & \sin 2\upsilon & 0 & \cos 2\upsilon & 0 \\ 0 & 0 & 0 & \sin\upsilon & 0 & \cos\upsilon \end{bmatrix}. \tag{12}$$

Using equation 10, we may combine the tilted angle and the stiffness matrix of the tilted TI medium to calculate the stiffness matrix of the corresponding VTI medium. Substituting the calculated stiffness matrix of the VTI medium into equations 2-5, we obtain the polarization and azimuth angles of P- and SV-waves. Base on the linear slip theory, the stiffness matrix of the HTI medium is given by (Schoenberg and Douma, 1988; Schoenberg and Sayers, 1995; Gurevich, 2003)

$$\mathbf{C}_{\mathrm{HTI}} = \begin{bmatrix} (\lambda{+}2\mu)(1-\Delta_N) & \lambda(1-\Delta_N) & \lambda(1-\Delta_N) & 0 & 0 & 0 \\ \lambda(1-\Delta_N) & (\lambda{+}2\mu)\left(1-\chi^2\Delta_N\right) & \lambda(1-\chi\Delta_N) & 0 & 0 & 0 \\ \lambda(1-\Delta_N) & \lambda(1-\chi\Delta_N) & (\lambda{+}2\mu)\left(1-\chi^2\Delta_N\right) & 0 & 0 & 0 \\ 0 & 0 & 0 & \mu & 0 & 0 \\ 0 & 0 & 0 & 0 & \mu(1-\Delta_T) & 0 \\ 0 & 0 & 0 & 0 & 0 & \mu(1-\Delta_T) \end{bmatrix}, \tag{13}$$

where λ and μ are Lamé constants of the homogeneous isotropic host rock, $\chi = \dfrac{\lambda}{\lambda{+}2\mu}$, and Δ_N and Δ_T are the normal and tangential fracture weaknesses related to fracture properties (e.g. fracture density and fracture fillings).

Combining Hudson (1980) penny-shaped crack model and the linear slip theory, Bakulin et al. (2000) presented expressions of fracture weaknesses in terms of fracture property

$$\begin{aligned} \Delta_N &= \frac{4e}{3g(1-g)\left[1+\dfrac{1}{\pi(1-g)}\left(\dfrac{k'+4/3\mu'}{\mu\psi}\right)\right]}, \\ \Delta_T &= \frac{16e}{3(3-2g)\left[1+\dfrac{4}{\pi(3-2g)}\left(\dfrac{\mu'}{\mu\psi}\right)\right]}, \end{aligned} \tag{14}$$

where e is fracture density, ψ is fracture aspect ratio, and k' and μ' are bulk and shear moduli of fillings in fractures, respectively.

Assuming the tilted angle υ being $\pi/2$, we first use the stiffness matrix of the HTI medium to express the VTI medium in terms of the normal and tangential fracture weaknesses

$$\mathbf{C}_{\text{VTI}} = \begin{bmatrix} (\lambda{+}2\mu)\left(1-\chi^2\Delta_N\right) & \lambda\left(1-\chi\Delta_N\right) & \lambda\left(1-\Delta_N\right) & 0 & 0 & 0 \\ \lambda\left(1-\chi\Delta_N\right) & (\lambda{+}2\mu)\left(1-\chi^2\Delta_N\right) & \lambda\left(1-\Delta_N\right) & 0 & 0 & 0 \\ \lambda\left(1-\Delta_N\right) & \lambda\left(1-\Delta_N\right) & (\lambda{+}2\mu)\left(1-\Delta_N\right) & 0 & 0 & 0 \\ 0 & 0 & 0 & \mu\left(1-\Delta_T\right) & 0 & 0 \\ 0 & 0 & 0 & 0 & \mu\left(1-\Delta_T\right) & 0 \\ 0 & 0 & 0 & 0 & 0 & \mu \end{bmatrix}. \tag{15}$$

Substituting equation 15 into equation 10, we finally obtain the stiffness parameters of the TTI medium

$$\begin{aligned} C_{11} =& (\lambda{+}2\mu)\left(1-\chi^2\Delta_N\right)\cos^4\upsilon{+}\frac{1}{2}\lambda\left(1-\Delta_N\right)(\sin 2\upsilon)^2 \\ &+ (\lambda{+}2\mu)\left(1-\Delta_N\right)\sin^4\upsilon + \mu\left(1-\Delta_T\right)(\sin 2\upsilon)^2, \end{aligned}$$

$$C_{12} = \lambda\left(1-\chi\Delta_N\right)\cos^2\upsilon{+}\lambda\left(1-\Delta_N\right)\sin^2\upsilon,$$

$$\begin{aligned} C_{13} =& \frac{1}{4}(\lambda{+}2\mu)\left(1-\chi^2\Delta_N\right)(\sin 2\upsilon)^2{+}\lambda\left(1-\Delta_N\right)\sin^4\upsilon + \lambda\left(1-\Delta_N\right)\cos^4\upsilon \\ &+ \frac{1}{4}(\lambda{+}2\mu)\left(1-\Delta_N\right)(\sin 2\upsilon)^2 - \mu\left(1-\Delta_T\right)(\sin 2\upsilon)^2, \end{aligned}$$

$$C_{14} = 0,$$

$$\begin{aligned} C_{15} =& (\lambda{+}2\mu)\left(1-\chi^2\Delta_N\right)\sin\upsilon\cos^3\upsilon{+}\lambda\left(1-\Delta_N\right)\sin^3\upsilon\cos\upsilon \\ &- \lambda\left(1-\Delta_N\right)\sin\upsilon\cos^3\upsilon - (\lambda{+}2\mu)\left(1-\Delta_N\right)\sin^3\upsilon\cos\upsilon - \mu\left(1-\Delta_T\right)\sin 2\upsilon\cos 2\upsilon, \end{aligned}$$

$$C_{16} = 0,$$

$$C_{21} = \lambda\left(1-\chi\Delta_N\right)\cos^2\upsilon + \lambda\left(1-\Delta_N\right)\sin^2\upsilon, C_{22} = (\lambda{+}2\mu)\left(1-\chi^2\Delta_N\right),$$

$$C_{23} = \lambda\left(1-\chi\Delta_N\right)\sin^2\upsilon + \lambda\left(1-\Delta_N\right)\cos^2\upsilon, C_{24} = 0,$$

$$C_{25} = \lambda\left(1-\chi\Delta_N\right)\left(\frac{1}{2}\sin 2\upsilon\right) - \lambda\left(1-\Delta_N\right)\left(\frac{1}{2}\sin 2\upsilon\right), C_{26} = 0,$$

$$C_{31} = \frac{1}{4}(\lambda{+}2\mu)\left(1-\chi^2\Delta_N\right)(\sin 2\upsilon)^2 + \lambda(1-\Delta_N)\cos^4\upsilon + \lambda(1-\Delta_N)\sin^4\upsilon + \frac{1}{4}(\lambda{+}2\mu)(1-\Delta_N)(\sin 2\upsilon)^2,$$

$$C_{32} = \lambda(1-\chi\Delta_N)\sin^2\upsilon + \lambda(1-\Delta_N)\cos^2\upsilon,$$

$$C_{33} = (\lambda{+}2\mu)\left(1-\chi^2\Delta_N\right)\sin^4\upsilon + \frac{1}{2}\lambda(1-\Delta_N)(\sin 2\upsilon)^2 + (\lambda{+}2\mu)(1-\Delta_N)\cos^4\upsilon,$$

$$C_{34} = 0,$$

$$C_{35} = (\lambda{+}2\mu)\left(1-\chi^2\Delta_N\right)\sin^3\upsilon\cos\upsilon + \lambda(1-\Delta_N)\sin\upsilon\cos^3\upsilon - \lambda(1-\Delta_N)\sin^3\upsilon\cos\upsilon - (\lambda{+}2\mu)(1-\Delta_N)\sin\upsilon\cos^3\upsilon,$$

$$C_{36} = 0, C_{41} = 0, C_{42} = 0, C_{43} = 0, C_{44} = \mu - \mu\Delta_T\cos^2\upsilon, C_{45} = 0, C_{46} = \mu\Delta_T\sin\upsilon\cos\upsilon,$$

$$C_{51} = (\lambda{+}2\mu)\left(1-\chi^2\Delta_N\right)\sin\upsilon\cos^3\upsilon - \lambda(1-\Delta_N)\sin\upsilon\cos^3\upsilon - 2\mu(1-\Delta_N)\sin^3\upsilon\cos\upsilon - \mu(1-\Delta_T)\cos 2\upsilon\sin 2\upsilon,$$

$$C_{52} = \frac{1}{2}\lambda(1-\chi\Delta_N)\sin 2\upsilon - \frac{1}{2}\lambda(1-\Delta_N)\sin 2\upsilon,$$

$$C_{53} = (\lambda{+}2\mu)\left(1-\chi^2\Delta_N\right)\sin^3\upsilon\cos\upsilon - \lambda(1-\Delta_N)\sin^3\upsilon\cos\upsilon - 2\mu(1-\Delta_N)\sin\upsilon\cos^3\upsilon + \mu(1-\Delta_T)\cos 2\upsilon\sin 2\upsilon,$$

$$C_{54} = 0,$$

$$C_{55} = \frac{1}{4}(\lambda{+}2\mu)\left(1-\chi^2\Delta_N\right)(\sin 2\upsilon)^2 + \frac{1}{4}(\lambda{+}2\mu)(1-\Delta_N)(\sin 2\upsilon)^2 - \frac{1}{2}\lambda(1-\Delta_N)(\sin 2\upsilon)^2 + \mu(1-\Delta_T)(\cos 2\upsilon)^2,$$

$$C_{56} = 0, C_{61} = 0, C_{62} = 0, C_{63} = 0,$$

$$C_{64} = \mu\Delta_T\sin\upsilon\cos\upsilon, C_{65} = 0, C_{66} = \mu - \mu\Delta_T\sin^2\upsilon. \tag{16}$$

Transmission angles of P-and SV-waves in TTI media

Snell′s law is employed to calculate reflection and transmission angles of P-and S-waves in homogenous isotropic media. A generalized form of Snell′s law in anisotropic media is proposed by Slawinski (1996) and Slawinski et al. (2000). Figure 2 shows reflection and transmission of P-and SV-waves for the case of an interface separating isotropic and anisotropic layers. The expression of Snell′s law extended to TTI media under the

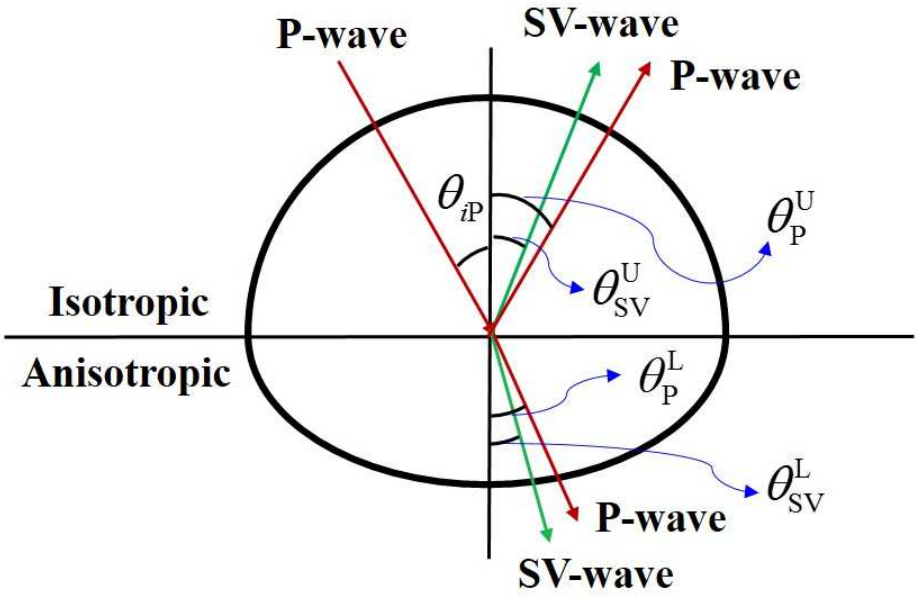

FIG. 2. Reflection and transmission angles of P-and SV-waves. The parameter $\theta_{i\mathrm{P}}$ is P-wave incident angle, $\theta_{\mathrm{P}}^{\mathrm{U}}$ and $\theta_{\mathrm{SV}}^{\mathrm{U}}$ are reflection angles of P-and SV-waves in the upper isotropic layer, and $\theta_{\mathrm{P}}^{\mathrm{L}}$ and $\theta_{\mathrm{SV}}^{\mathrm{L}}$ are transmission angles of P-and SV-waves in the lower anisotropic layer.

assumption of an isotropic upper layer is given by

$$\frac{\sin\left(\theta_{i\mathrm{P}}\right)}{V_{\mathrm{P}}^{\mathrm{U}}}=\frac{\sin\left(\theta_{\mathrm{P}}^{\mathrm{U}}\right)}{V_{\mathrm{P}}^{\mathrm{U}}}=\frac{\sin\left(\theta_{\mathrm{SV}}^{\mathrm{U}}\right)}{V_{\mathrm{SV}}^{\mathrm{U}}}=\frac{\sin\left(\theta_{\mathrm{P}}^{\mathrm{L}}\right)}{V_{\mathrm{P}}^{\mathrm{L}}\left(\theta_{\mathrm{P}}^{\mathrm{L}},\phi\right)}=\frac{\sin\left(\theta_{\mathrm{SV}}^{\mathrm{L}}\right)}{V_{\mathrm{SV}}^{\mathrm{L}}\left(\theta_{\mathrm{SV}}^{\mathrm{L}},\phi\right)}=K, \tag{17}$$

where $V_{\mathrm{P}}^{\mathrm{U}}$ and $V_{\mathrm{SV}}^{\mathrm{U}}$ are P-and SV-wave velocities of the upper layer,$V_{\mathrm{P}}^{\mathrm{L}}\left(\theta_{\mathrm{P}}^{\mathrm{L}},\phi\right)$ and $V_{\mathrm{SV}}^{\mathrm{L}}\left(\theta_{\mathrm{SV}}^{\mathrm{L}},\phi\right)$ are P-and SV-wave velocities of the lower layer, which are related to the corresponding transmission angle and azimuth, and K is ray parameter.

The P-and SV-wave velocities of the lower layer are expressed as

$$\begin{aligned}
V_{\mathrm{P}}^{\mathrm{L}}&=\sqrt{\frac{1}{2\rho}\left[\left(C_{11}^{\mathrm{V}}+C_{44}^{\mathrm{V}}\right)\left(E^{2}+F^{2}\right)+\left(C_{33}^{\mathrm{V}}+C_{44}^{\mathrm{V}}\right)G^{2}+\sqrt{D}\right]},\\
V_{\mathrm{SV}}^{\mathrm{L}}&=\sqrt{\frac{1}{2\rho}\left[\left(C_{11}^{\mathrm{V}}+C_{44}^{\mathrm{V}}\right)\left(E^{2}+F^{2}\right)+\left(C_{33}^{\mathrm{V}}+C_{44}^{\mathrm{V}}\right)G^{2}-\sqrt{D}\right]},
\end{aligned} \tag{18}$$

where ρ is the density, and the expressions of E, F, and D are shown in equation 3.

In practice, in order to estimate the transmission angles of P-and SV-waves, we first use the velocity of the upper isotropic layer to calculate ray parameters at different incident

angles, and then we estimate the transmission angles and velocities of P- and SV-waves using equations 17 and 18.

NUMERICAL SIMULATION

We construct a reflection interface (Figure 3) which separates isotropic and TTI layers to analyze how fracture property affects the exact reflection coefficient. For this model, we assume that elastic properties (P-and S-wave velocities, and density) of the upper isotropic layer are same to the background of the lower TTI layer, which means the reflection is induced by tilted fractures.

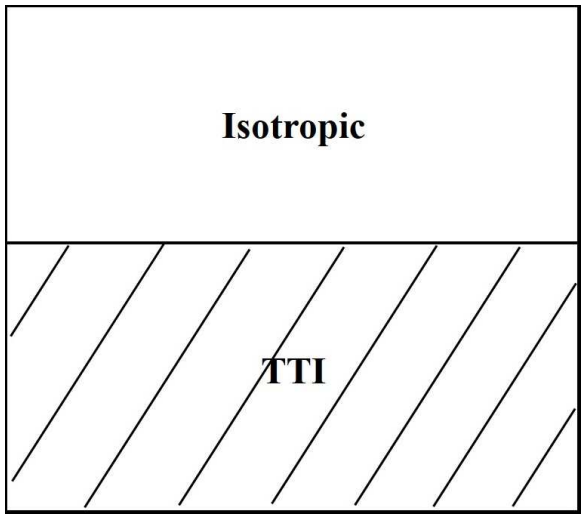

FIG. 3. An interface separating isotropic and TTI layers. P-and S-wave velocities of the isotropic layer and background of TTI layer are 3.81 $\mathrm{km/s}$, 2.59 $\mathrm{km/s}$, and 2.26 $\mathrm{g/cm^3}$, respectively.

Figure 4 plots PP-wave reflection coefficient for the case of different values of fracture density and tilted angle. We observe that in the case of HTI media (i.e. $\nu = 90^\circ$), the absolute value of PP-wave reflection coefficient increases with the fracture density and the variation of the reflection coefficient with the azimuthal angle for the case of a big fracture density is larger than that for the case of a small fracture density. However, the tilted angle may affect the value of the reflection coefficient. From Figure 5, we confirm that the tilted angle mainly affects the value of reflection coefficient, and its influence on the variation of reflection coefficient with the azimuthal angle is small.

CONCULISONS

Based on the linear slip theory, we express the stiffness matrix of VTI media in terms of the normal and tangential fracture weaknesses. Using the relationship between the matrices of VTI and TTI media, we derive explicit expressions of stiffness parameters that are related to fracture properties (fracture density and aspect ratio) and fluid parameters (bulk and shear moduli). We also show the method to compute the transmission angles of P- and SV-waves in TTI media using the extended Snell′s law. The step to obtain the exact solution of PP-wave reflection coefficient in reservoirs with tilted fractures involves: 1) calculate the stiffness matrix of HTI media given fracture properties and fluid parameters; 2) assume the tilted angle to be $\pi/2$ to compute the stiffness matrix of VTI media and then

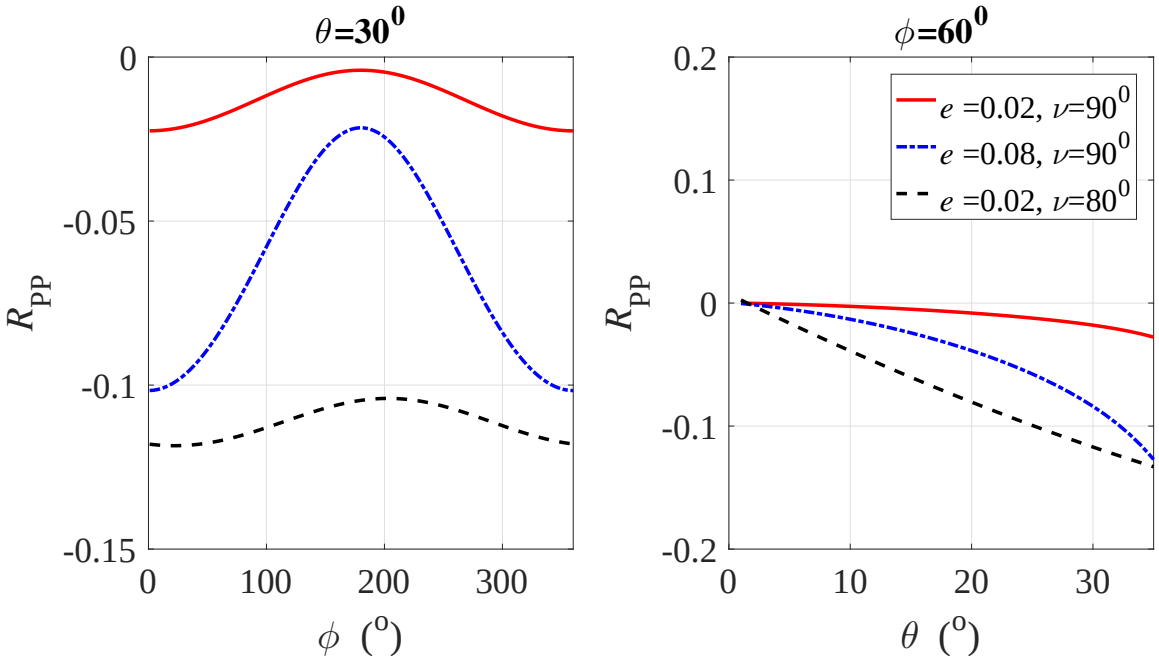

FIG. 4. Reflection coefficient variations with the incident angle θ and the azimuthal angle ϕ in the case of different values of fracture density and tilted angle.

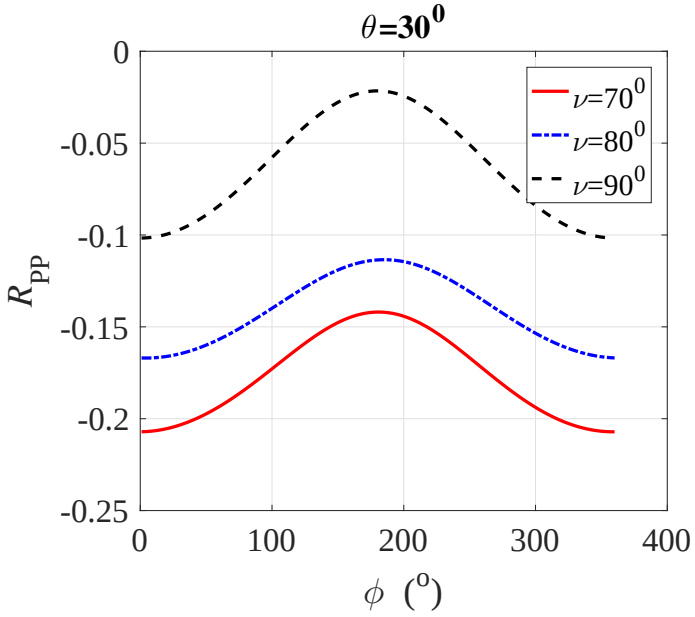

FIG. 5. Reflection coefficient variations with the azimuthal angle in the case of different values of tilted angle.

calculate the stiffness matrix of TTI media given a tilted angle; 3) compute the polarization and azimuthal angles of P- and S-waves using the calculated stiffness parameters of TTI media; and 4) obtain the exact result of PP-wave reflection coefficient by solving the extend Zoeppritz equation. Following this step, we finally model PP-wave reflection coefficient variations with the incidence angle and the azimuthal angle given different values of fracture density and tilted angle. We conclude that for the TI media with a relatively high tilted angle, the variation of the reflection coefficient with the azimuthal angle is mainly affected

by fracture density, while the tilted angle affects the value of the reflection coefficient.

ACKNOWLEDGEMENTS

The industrial sponsors of CREWES are thanked for their support. We gratefully acknowledge support from NSERC (Natural Science and Engineering Research Council of Canada) through the grant CRDPJ 461179-13. This research was undertaken thanks in part to funding from the Canada First Research Excellence Fund and Mitacs Project.

REFERENCES

Aki, K., and Richards, P. G., 2002, Quantitative seismology: University science books.

Alkhalifah, T., 1995, Efficient synthetic-seismogram generation in transversely isotropic, inhomogeneous media: Geophysics, **60**, No. 4, 1139–1150.

Alkhalifah, T., and Larner, K., 1994, Migration error in transversely isotropic media: Geophysics, **59**, No. 9, 1405–1418.

Auld, B. A., 1990, Acoustic fields and waves in solids: Krieger, Florida.

Avseth, P., Mukerji, T., and Mavko, G., 2010, Quantitative seismic interpretation: Applying rock physics tools to reduce interpretation risk: Cambridge university press.

Bakulin, A., Grechka, V., and Tsvankin, I., 2000, Estimation of fracture parameters from reflection seismic data–part i: Hti model due to a single fracture set: Geophysics, **65**, No. 6, 1788–1802.

Bakulin, A., Woodward, M., Nichols, D., Osypov, K., and Zdraveva, O., 2010, Building tilted transversely isotropic depth models using localized anisotropic tomography with well information: Geophysics, **75**, No. 4, D27–D36.

Behera, L., and Tsvankin, I., 2009, Migration velocity analysis for tilted transversely isotropic media: Geophysical Prospecting, **57**, No. 1, 13–26.

Berryman, J. G., Grechka, V. Y., and Berge, P. A., 1999, Analysis of thomsen parameters for finely layered vti media: Geophysical Prospecting, **47**, No. 6, 959–978.

Carcione, J. M., 1992, Anisotropic q and velocity dispersion of finely layered media: Geophysical Prospecting, **40**, No. 7, 761–783.

Carcione, J. M., 2000, A model for seismic velocity and attenuation in petroleum source rocks: Geophysics, **65**, No. 4, 1080–1092.

Chen, H., Zhang, G., Chen, J., and Yin, X., 2014, Fracture filling fluids identification using azimuthally elastic impedance based on rock physics: Journal of Applied Geophysics, **110**, 98–105.

Chen, H., Zhang, G., Chen, T., and Yin, X., 2017, Joint pp-and psv-wave amplitudes versus offset and azimuth inversion for fracture compliances in horizontal transversely isotropic media: Geophysical Prospecting, In press.

Fletcher, R. P., Du, X., and Fowler, P. J., 2009, Reverse time migration in tilted transversely isotropic (tti) media: Geophysics, **74**, No. 6, WCA179–WCA187.

Grechka, V., Pech, A., Tsvankin, I., and Han, B., 2001, Velocity analysis for tilted transversely isotropic media: A physical modeling example: Geophysics, **66**, No. 3, 904–910.

Gurevich, B., 2003, Elastic properties of saturated porous rocks with aligned fractures: Journal of Applied Geophysics, **54**, No. 3, 203–218.

Hudson, J., 1980, Overall properties of a cracked solid: Mathematical Proceedings of the Cambridge Philosophical Society, **88**, No. 2, 371–384.

Nadri, D., Sarout, J., Bóna, A., and Dewhurst, D., 2012, Estimation of the anisotropy parameters of transversely isotropic shales with a tilted symmetry axis: Geophysical Journal International, **190**, No. 2, 1197–1203.

Pšenčík, I., and Gajewski, D., 1998, Polarization, phase velocity, and nmo velocity of qp-waves in arbitrary weakly anisotropic media: Geophysics, **63**, No. 5, 1754–1766.

Pšenčík, I., and Vavryčuk, V., 1998, Weak contrast pp wave displacement r/t coefficients in weakly anisotropic elastic media: Pure and Applied Geophysics, **151**, No. 2-4, 699–718.

Rüger, A., 1996, Reflection coefficients and azimuthal avo analysis in anisotropic media.: Ph.D. thesis, Colorado School of Mines.

Schoenberg, M., and Douma, J., 1988, Elastic wave propagation in media with parallel fractures and aligned cracks: Geophysical Prospecting, **36**, No. 6, 571–590.

Schoenberg, M., and Protázio, J., 1992, ′zoeppritz′rationalized and generalized to anisotropy: Journal of seismic exploration, **1**, No. S1, 125–144.

Schoenberg, M., and Sayers, C. M., 1995, Seismic anisotropy of fractured rock: Geophysics, **60**, No. 1, 204–211.

Sheriff, R. E., and Geldart, L. P., 1995, Exploration seismology: Cambridge university press.

Shragge, J., 2016, Acoustic wave propagation in tilted transversely isotropic media: Incorporating topography: Geophysics.

Shuey, R., 1985, A simplification of the zoeppritz equations: Geophysics, **50**, No. 4, 609–614.

Slawinski, M. A., 1996, On elastic-wave propagation in anisotropic media: reflection/refraction laws, raytracing, and travel time inversion: Ph.D. thesis, University of Calgary.

Slawinski, M. A., Slawinski, R. A., Brown, R. J., and Parkin, J. M., 2000, A generalized form of snell′s law in anisotropic media: Geophysics, **65**, No. 2, 632–637.

Stovas, A., and Alkhalifah, T., 2013, Mapping of moveout in tilted transversely isotropic media: Geophysical Prospecting, **61**, No. 6, 1171–1177.

Stovas, A., Landrø, M., and Avseth, P., 2006, Avo attribute inversion for finely layered reservoirs: Geophysics, **71**, No. 3, C25–C36.

Thomsen, L., 1986, Weak elastic anisotropy: Geophysics, **51**, No. 10, 1954–1966.

Thomsen, L., 1988, Reflection seismology over azimuthally anisotropic media: Geophysics, **53**, No. 3, 304–313.

Tsvankin, I., 1997, Anisotropic parameters and p-wave velocity for orthorhombic media: Geophysics, **62**, No. 4, 1292–1309.

Wang, H., and Peng, S., 2015, Reflection coefficient of qp, qs and sh at a plane boundary between viscoelastic tti media: Geophysical Journal International, **204**, No. 1, 555–568.

Wang, X., and Tsvankin, I., 2013, Ray-based gridded tomography for tilted transversely isotropic media: Geophysics.